

# Use of temporal patterns in vapor pressure deficit to explain spatial autocorrelation dynamics in tree transpiration

JONATHAN D. ADELMAN,<sup>1</sup> BRENT E. EWERS<sup>1,2</sup> and D. SCOTT MACKAY<sup>3</sup>

<sup>1</sup> Department of Botany, University of Wyoming, Laramie, WY 82071, USA

<sup>2</sup> Corresponding author (beewers@uwyo.edu)

<sup>3</sup> Department of Geography, State University of New York, Buffalo, NY, USA

Received May 3, 2007; accepted June 18, 2007; published online February 1, 2008

**Summary** To quantify the relationship between temporal and spatial variation in tree transpiration, we measured sap flow in 129 trees with constant-heat sap flow sensors in a subalpine forest in southern Wyoming, USA. The forest stand was located along a soil water gradient from a stream side to near the top of a ridge. The stand was dominated by *Pinus contorta* Dougl. ex Loud. with *Picea engelmannii* Parry ex Engelm and *Abies lasiocarpa* (Hook.) Nutt. present near the stream and scattered individuals of *Populus tremuloides* Michx. throughout the stand. We used a cyclic sampling design that maximized spatial information with a minimum number of samples for semivariogram analyses. All species exhibited previously established responses to environmental variables in which the dominant driver was a saturating response to vapor pressure deficit ( $D$ ). This response to  $D$  is predictable from tree hydraulic theory in which stomatal conductance declines as  $D$  increases to prevent excessive cavitation. The degree to which stomatal conductance declines with  $D$  is dependent on both species and individual tree physiology and increases the variability in transpiration as  $D$  increases. We quantified this variability spatially by calculating the spatial autocorrelation within 0.2-kPa  $D$  bins. Across 11 bins of  $D$ , spatial autocorrelation in individual tree transpiration was inversely correlated to  $D$  and dropped from 45 to 20 m. Spatial autocorrelation was much less for transpiration per unit leaf area and not significant for transpiration per unit sapwood area suggesting that spatial autocorrelation within a particular  $D$  bin could be explained by tree size. Future research should focus on the mechanisms underlying tree size spatial variability, and the potentially broad applicability of the inverse relationship between  $D$  and spatial autocorrelation in tree transpiration.

**Keywords:** geostatistics, sapwood area, scaling, tree hydraulics.

## Introduction

Scaling from more easily measured quantities to those more difficult to measure constitutes one of the fundamental problems in ecology. A traditional approach to scaling has been to

use a connection between space and time such that an increase in temporal scale would lead directly to an increase in spatial scale (Jarvis 1995). Thus, hypotheses posed at a certain spatial domain are often constrained to temporal domains of an equivalent scale, and may overlook processes occurring at different spatiotemporal scales (Chang et al. 2006). Overcoming this constraint is a prerequisite for detailed studies of the causes and extent of spatial and temporal variations in ecological patterns and processes (Levin 1992).

An assumption underlying ecological studies that do not explicitly quantify spatial autocorrelation is that sampled points in geographic space are stochastically independent of each other. This assumption is necessary to perform classical statistical tests of hypotheses (Sokal and Rohlf 1995). Ecosystems rarely behave accordingly, and spatial autocorrelation is a common characteristic in nature. Spatial autocorrelation can be defined as the degree of relatedness between values of random variables, at pairs of locations a certain distance apart (Legendre 1993). This property occurs at virtually all scales: spatial autocorrelation has been observed at the genetic level (Conti and Witte 2003); in bacterial (Franklin et al. 2002) and fungal (Morris 1999) populations; in soils (Webster and de la Cuanalo 1975, Schlesinger et al. 1996, Western et al. 1998, Anderson et al. 2004), with distribution of macronutrients (Jackson and Caldwell 1993); in plant communities (Robertson 1987); and across mountain ranges (Bishop et al. 2003).

These studies show that ignoring an ecological variable's spatial structure leads to a potential oversimplification of the ecosystem being studied. Spatial heterogeneity is a functional component in ecosystems, and not merely noise generated from a random process (Legendre 1993). Ecosystems contain spatial structure, and quantifying these spatial components with tools such as geostatistics is crucial when trying to understand ecosystem composition and function (Legendre and Legendre 1998, Neuhauser 2001). An example of such spatial structure occurs across a hill slope where variation in water availability changes ecosystem water fluxes through effects on tree transpiration (Tromp-van Meerveld and McDonnell 2006).

Transpiration is a key physiological process whose mea-

surement suffers the above scaling constraints. Mechanistic understanding of transpiration varies with temporal and spatial scales. Stomata serve as the pathway of carbon gain from photosynthesis and water loss from transpiration, and their behavior is intricately tied to both processes (Jarvis 1976, Farquhar and Wong 1984, Ball et al. 1987, Tardieu and Davies 1993, Leuning 1995, Dewar 2002). Transpiration exhibits a diurnal cycle driven by environmental parameters such as vapor pressure deficit ( $D$ ) and photosynthetically active radiation ( $Q$ ) (Schulze et al. 1985, Monteith 1995). The relationship between transpiration and  $D$  can be understood using Darcy's and Fick's Laws (Scheidegger 1974, Whitehead and Jarvis 1981), in which transpiration rate is driven by  $D$  externally (Mott and Parkhurst 1991) and limited internally by the product of hydraulic conductivity ( $K$ ) and the water potential between leaves and soil. Because  $K$  is not constant but decreases as transpiration increases in response to cavitations (Sperry et al. 1998), a saturating relationship between transpiration and  $D$  results as stomata close to prevent excessive cavitation (Sperry et al. 1998, Ewers et al. 2005).

Transpiration is measured and analyzed at a variety of scales to interpret biological functions and environmental drivers. Sap flow per unit conducting sapwood area ( $J_S$ ) is a commonly used measure of transpiration (Čermák 1995, Wullschlegel et al. 1998, Oren et al. 1998). Transpiration is often scaled to the whole crown ( $E_C$ ) to determine whole ecosystem water use or expressed per unit leaf area ( $E_L$ ) to explain differences in  $E_C$  caused by effects of environment or species, or both, on biomass partitioning between sapwood ( $A_S$ ) and leaf ( $A_L$ ) area (McDowell et al. 2002). However, uncertainties remain about how to scale sap flow estimates of  $E_C$  and  $E_L$  temporally and spatially from point measurements of sap flow in the main stem or leaf- and branch-level measurements to the whole tree. Various smoothing and modeling techniques are needed to remove temporal variability in  $J_S$  that is unrelated to plant hydraulics (Zweifel et al. 2002, Ewers et al. 2007).

To test these ideas on ecological scaling, we quantified tree transpiration across a potential hill-slope soil water gradient in the Medicine Bow Mountains of Wyoming, taking advantage of the rich history of ecological studies in this area. Previous ecological work in this and surrounding areas includes studies on evapotranspiration (Fetcher 1976, Running 1980a, 1980b, Knight et al. 1981, Kaufmann 1985), species effects on stand transpiration (Pataki et al. 2000), photosynthesis (Day et al. 1987, Carter and Smith 1988), succession (Knapp and Smith 1981), stomatal dynamics (Smith et al. 1984), spatial variability in soil characteristics (Rahman et al. 1996) and nutrient outflow from contrasting ecosystems (Knight et al. 1985). Tree transpiration in pure lodgepole pine (*Pinus contorta* Dougl.) forests has been estimated to be 50–60% of evapotranspiration (Knight et al. 1985). Thus, systematic variation in  $E_C$  of these mountainous forests with hill-slope variation has important implications for estimates of evapotranspiration from mass balance estimates based on the assumption that one or a small group of plots is representative of the stand (Oren et al. 1998).

Our main objective was to bridge the knowledge gap between traditional ecophysiological research in this well-studied mountain range and spatially explicit methods, thereby attempting to escape the supposed constraints on both spatial and temporal domains, and ultimately to determine patterns and processes associated with spatial variation inherent in transpiration. We measured transpiration in a mixed-species subalpine forest across a hill slope during the driest part of the season when soil water content is nearly always limiting throughout the stand (Pataki et al. 2000). Our study builds on recent hill-slope transpiration measurements (Tromp-van Meerveld and McDowell 2006) by having a sufficient sample size to explicitly analyze spatial autocorrelation in transpiration. Specific hypotheses tested were: (1) spatial autocorrelation exists in tree transpiration; (2) spatial autocorrelation of tree transpiration varies temporally; and (3)  $D$  or  $Q$  drives temporal dynamics in this spatial autocorrelation.

## Methods

### Site description

The study was conducted in a mixed species forest on a south-facing hill slope rising from the south fork of Mill's Creek, in the Medicine Bow Mountains of southeastern Wyoming, USA (41°22'15" N, 106°08'00" W, NAD83, USGS Centennial quad, elevation about 3000 m). The climate is characterized by long cold winters and short cool summers: mean daytime temperature in July is about 20 °C. Snow often begins to accumulate by the end of October, and stands are usually not snow free until June. Total precipitation ranges from 41 to 90 cm with about 70% occurring as snow (Knight et al. 1985).

The hill slope is 150–200 m in length from stream side to ridge top, with a mean slope of 36%. The lower portion of the hill slope was defined as the region of the slope with a visibly higher proportion of subalpine fir (*Abies lasiocarpa* (Hook.) Nutt.) and Engelmann spruce (*Picea engelmannii* Parry ex Englem) and lower proportion of trembling aspen (*Populus tremuloides* Michx.) and lodgepole pine (*Pinus contorta* Dougl. ex Loudon.). At this elevation, *A. lasiocarpa* and *P. engelmannii* are both more dominant in riparian areas (Knapp and Smith 1981). The upper portion was defined as the region dominated by *P. contorta*, with individuals of the other three species usually not canopy dominants (Table 1). Division of the hill slope into two portions also accorded with soil water measurements (see below). The soil is an incepticol with weakly developed horizons. Measured trees varied in diameter at breast height (DBH) from 3.4 to 47.0 cm. Numbers of measured trees per species, as well as mean density, leaf area, basal area and sapwood area are listed in Table 1.

### Sampling design

A cyclic sampling design that maximized spatial information with a minimum number of samples (Burrows et al. 2002) was used to determine the location of plots. A cycle is the number of fundamental lengths taken before the sampling pattern repeats. For each cycle length, an optimum spacing is estab-

Table 1. Tree species sample size ( $n$ ), tree density (no. ha<sup>-1</sup>), mean leaf area ( $A_L$ ) per unit ground area, mean basal area ( $A_B$ ; m<sup>2</sup> ha<sup>-1</sup>) and mean sapwood area ( $A_S$ ; m<sup>2</sup> ha<sup>-1</sup>).

Species	$n$	Density	$A_L$	$A_B$	$A_S$
<i>Pinus contorta</i>	54	866	1.1	24.7	11.0
<i>Abies lasiocarpa</i>	37	825	0.9	7.4	1.2
<i>Picea engelmannii</i>	11	157	0.2	2.6	2.1
<i>Populus tremuloides</i>	27	414	0.3	4.9	3.5

lished that provides sample pairs separated by any distance for spatial statistical analysis. For instance, a 3/7 cyclic design measures three plots out of every seven plots in one dimension. The three plots are spaced within a cycle that repeats. The first plot pair is at a unit distance of one, whereas the second and third plots are at two and plots one and four are at a unit distance of three. Unit distance four is established when the cycle repeats between plot four of the first cycle and plot one of the second cycle. Further unit distances are then a result of how many cycle repeats are made.

Basal areas ( $A_B$ ) of trees and plots of varying size were measured in a preliminary study in May–June 2003 (no sap flow measurements were conducted during this time), to estimate the scale at which spatial patterns of transpiration were likely to occur to establish the cycle length of sap flow measurements in 2004. Basal area is easily measured, and can be considered a proxy for sapwood area ( $A_S$ ), which is a component of transpiration. Based on the initial  $A_B$  measurements, a 4-m radius for each plot was deemed appropriate. A 4/9 cycle definition (four plots were measured out of every nine) was used to populate north–south transects, and a 3/7 (three plots were measured out of every seven) cycle definition was used for east–west transects, creating a 176 × 80 m array of plot centers (Figure 1). Two sampling strategies were used at various plot centers in the array. Three plots for intensive study were selected in lower-, mid- and upper-slope positions. However, the plots were grouped into only upper- and lower-slope positions after preliminary analyses showed that trees in the mid and lower slopes were not significantly different. To represent the entire range of diameter classes, we measured  $J_S$  in eight *P. contorta* trees in the mid- and upper-slope positions and in four trees of each species in the lower-slope position. Data from the intensively studied plots were used to determine the relationship between traditional sap flow plots (e.g., Oren et al. 1998) and a spatially explicit sap flow sampling. Forty-five additional extensive plots were arranged according to the cycle lengths described above and DBH was measured for all trees. In each extensive plot,  $J_S$  was measured in the largest tree and in one randomly picked tree in the plot. If the largest tree was *P. contorta*, then we sampled at least one of the other species in the plot if available. Altogether, we sampled 129 trees across both extensive and intensive plots (Table 1). Plot sampling was ultimately only a device with which to pick individual trees, optimized for spatial analysis, for the biomass and sap flow measurements.

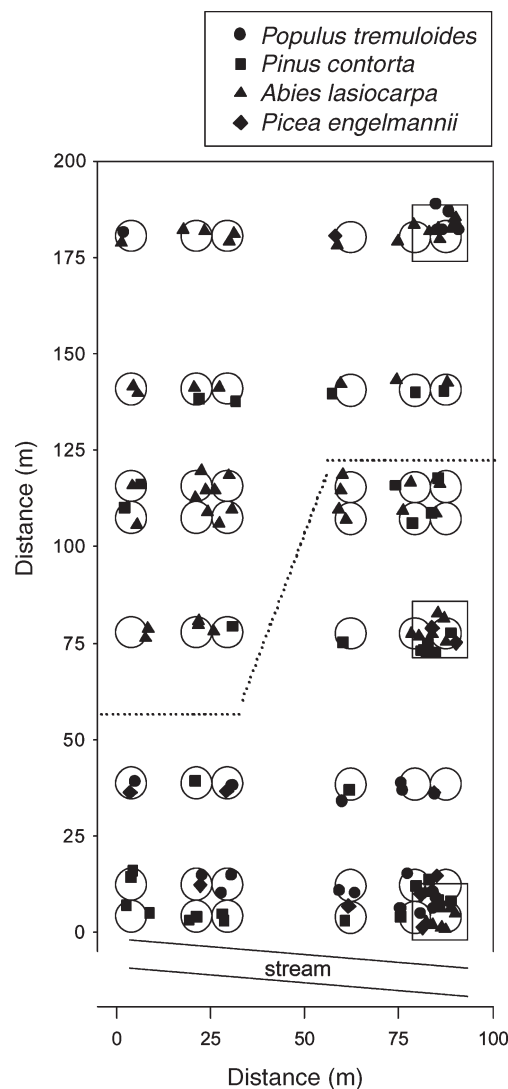


Figure 1. Map of study site showing intensive plots (squares), extensive plots (circles), stream and distance in meters between points. Each tree measured for sap flow is given a symbol representing its species. Plots below the dashed line indicate lower slope plots (which include the middle intensive plot because preliminary analyses showed no differences) and plots above the dashed line indicate upper slope plots.

#### Calculation of $A_S$ and $A_L$

The DBH of all trees selected for sap flow measurements was measured in October 2004 after completion of the sap flow sampling (see below). Concurrently, the same trees were cored and sapwood depth estimated visually. Sapwood area was calculated from sapwood depth, bark depth and DBH, and site- and species-specific allometric regressions between outside bark diameter and sapwood depth from cambium to heartwood. Sapwood areas were then calculated for each tree based on outside bark DBH measurements. Leaf area was obtained from general allometric equations relating  $A_S$  to  $A_L$  for each species from a local study encompassing the entire size range of trees in this study (Kaufmann and Troendle 1981).

### Measuring sap flow rate and transpiration

For each species in the intensively studied plots, sap flow was measured with constant-heat sap flow sensors (Granier 1987, Granier et al. 1996) in randomly chosen trees representing the range of available diameters. In the extensive plots, the largest tree of each species sampled was chosen to minimize confounding effects from subdominant canopy classes. Sapwood depth measurements indicated that the 20 mm sensors used accounted for, on average, more than 75% of the sapwood depth. Sap flow values were corrected based on sensor length and sapwood depth according to Clearwater et al. (1999). Transpiration values were calculated (Pataki et al. 2000) as:

$$E_L = \frac{J_s A_s}{A_L} \quad (1)$$

$$E_C = J_s A_s \quad (2)$$

Values of  $E_C$  and  $E_L$  were calculated on a per tree basis. All analyses were performed per tree and not per plot.

Instruments depended on solar power which was insufficient to complete all measurements on many days. Thus, sap flow data on only 8 days (August 6, September 2–4, 11 and 16–18) were used. Rain days were also removed because of their effects on sap flow measurements. In the late summer, convective storms rarely supply enough precipitation to equal canopy and litter interception and increase soil water content (Knight et al. 1985).

### Environmental variables

The mid-slope intensive plot contained a 12-m tower with a relative humidity and temperature probe (HMP 45C, Vaisala Instruments, Vantaa, Finland) from which half-hourly  $D$  was calculated, and a radiometer (Q7.1, REBS, Seattle, WA) used to measure net radiation. Because of sensor failure, we obtained only limited data for net radiation, and therefore established a linear relationship between these data and hourly incoming photosynthetically active radiation ( $Q$ ) obtained from the Clean Air Status and Trends Network database for a site about 5 km from the hill slope (<http://www.epa.gov/castnet>;  $r^2 = 0.88$ ,  $P < 0.01$ ). Surface (0–6 cm) soil water content (Theta Probe, Delta-T) was measured 11 times during the growing season of 2004 (June 15, 23, July 17, August 6, 19, 24, 25, September 1, 2, 11 and 16) at all extensive plot centers.

### Data reduction

Not all temporal variation in sap flow is due to environmental drivers (Ewers et al. 2007). Binning within a particular value of an environmental driver removes some of this temporal variation and allows more detailed analyses of spatial patterns. Because  $Q$  and  $D$  are correlated when  $Q$  is lagged with respect to  $D$  by 60 min ( $r^2 = 0.83$ ,  $P < 0.01$ ) and plant responses to  $D$  can be predicted from plant hydraulics in these species (Pataki et al. 2000),  $D$  was chosen for the binning procedure. Based on the corresponding recorded  $D$ , all half-hourly transpiration data were grouped into 0.2-kPa ranges of  $D$ . The sap flow val-

ues were then averaged, giving a mean value for each tree for each range of  $D$ . All subsequent spatial analyses were conducted on the means.

### Statistics

Because measurements were collected to quantify spatial autocorrelation, the effect of spatial autocorrelation on standard errors was accounted for by a repeated measures analysis in space (Burrows et al. 2002).

### Geostatistical analyses

To investigate spatial patterns across the hill slope, we applied a semivariogram analysis to all of the spatially collected data. The semivariogram examines the relationship between distance and pairs of points ( $h$ ) and the semivariance for each distance ( $\gamma$ ) calculated as:

$$\gamma(h) = \frac{1}{2N(h)} \sum_{i=1}^{N(h)} (z(x_i + h) - z(x_i))^2 \quad (3)$$

where  $N$  is the number of observations at lag distance  $h$ ,  $x_i$  is the  $i$ th location and  $z$  is the data value (Cressie 1993, Schabenberger and Gotway 2004). Interpretation of the measured, or experimental, semivariograms requires a model fitted through the  $\gamma$  values at all  $h$  values. We fit three types of relationships, a spherical model, a linear model and a nugget model.

The spherical model was:

$$\gamma(h) = \begin{cases} C_0 + C \left( 1.5 \left( \frac{h}{A} \right) - 0.5 \left( \frac{h}{A} \right)^3 \right) & \text{for } h \leq A \\ C_0 + C & \text{for } h > A \end{cases} \quad (4)$$

where  $C_0$  is nugget variance,  $C$  is structural variance,  $(C_0 + C)$  is the sill and  $A$  is the range. Nugget is the amount of variation found at distance zero and indicates unsolved variance exists at a scale finer than that of the field samples, inherently high variability, or sampling error. Sill is the amount of variance that occurs at the distance beyond which samples are spatially independent. Range is the distance between point pairs at which the sill occurs and provides an index of the scale of spatial pattern in the variable of interest.

The linear model was:

$$\gamma(h) = C_0 + bh \quad (5)$$

where  $b$  is the ratio of the sill to the range. The nugget model was:

$$\gamma(h) = C_0 + C \quad \text{for all } h \quad (6)$$

A linear model indicates that the sampling area does not include a range at which a sill is reached. The nugget model indicates no significant spatial autocorrelation at the scales measured and that all points are independent. The 95% confidence

intervals ( $CI_{95}$ ) for the experimental semivariograms were calculated as (Cressie 1993, Burrows et al. 2002):

$$CI_{95} = 1.96 \frac{\sqrt{2}\gamma}{\sqrt{N}} \quad (7)$$

Because semivariograms are sensitive to extreme differences between point pairs (Isaaks and Srivastava 1989), we excluded trees from the analyses if they had all of the following characteristics (1) the tree was part of a point-pair in any given lag class's spatial variance that was at least two orders of magnitude larger than the mean semivariance, (2) this tree exhibited such behavior across four or more lag classes, and (3) this tree's  $A_S$  or midday mean sap flow ( $J_{Smid}$ ; calculated as the mean of half-hourly sap flow values recorded between 1100 and 1400 h) was in the 95th or higher percentile among those sampled (in the case of this study,  $A_S > 325.5 \text{ cm}^2$  or  $J_{Smid} > 38.7 \text{ g m}^{-2} \text{ s}^{-1}$ ). Kriging is a linear interpolation that allows predictions of unknown values in the study area based on information from measurements made at sample locations and thus provides a map of spatially variable processes. Point-kriging in this study was based on the work of Cressie (1993), Kaluzny et al. (1998) and Pinheiro and Bates (2000).

All semivariogram analyses, tests for anisotropy and Kriging procedures were conducted with GS+ (Gamma Design Software, Plainwell, MI). We tested for stationarity by analyzing drift and systematic trends in means and variance (Cressie 1993) and by visually verifying the presence of a sill (Legendre and Legendre 1998). The presence of anisotropy was tested based on the procedures detailed by Isaaks and Srivastava (1989). Briefly, angle tolerances for directional variograms were set at  $10^\circ$  based on the minimum angle that would still have sufficient point pairs to cover the entire spatial domain for a map of anisotropic semivariance. Maps of anisotropic semivariance were then analyzed for every semivariogram constructed in the study to test for anisotropy and determine the azimuth(s) of anisotropy if present. All experimental semivariograms were fitted by the weighted least squares approach of Cressie (1993) in which the regression was weighted by the initial range estimated by GS+ and the number of point pairs in each lag class.

## Results

### Species and hill-slope location effects on transpiration

The effect of species on transpiration depended on how transpiration was expressed (Table 2). Two-way analysis of variance showed that species effects were significant for  $E_C$  and  $E_L$  ( $P < 0.001$ ), whereas location (upper- versus lower-hill-slope position) and its interaction with species were never significant ( $P > 0.2$  for  $J_S$ ,  $E_C$  and  $E_L$ ). Although there was no effect of species on  $J_S$ ,  $E_C$  varied among species by a factor of four, with *P. tremuloides* having the lowest transpiration rate and *P. engelmannii* the highest. The effect of species was even more pronounced for  $E_L$ , with an order of magnitude difference between *A. lasiocarpa* (lowest) and *P. tremuloides* (high-

Table 2. Tree species mean separation for sap flow per unit sapwood area ( $J_S$ ), whole-tree transpiration ( $E_C$ ) and transpiration per unit leaf area ( $E_L$ ). Values in parenthesis are one standard error of the mean, and letters indicate significant differences at  $P \leq 0.05$ . Samples sizes are given in Table 1.

Species	$J_S$ ( $\text{g m}^{-2} \text{ s}^{-1}$ )	$E_C$ ( $\text{g tree}^{-1} \text{ s}^{-1}$ )	$E_L$ ( $\text{g m}^{-2} \text{ s}^{-1}$ )
<i>Pinus contorta</i>	14.7 (1.6) a	0.37 (0.04) a	33.4 (3.3) a
<i>Abies lasiocarpa</i>	13.7 (2.5) a	0.27 (0.05) abc	7.4 (1.4) b
<i>Picea Engelmannii</i>	12.8 (2.7) a	0.42 (0.09) bc	13.8 (2.9) c
<i>Populus tremuloides</i>	13.5 (8.1) a	0.10 (0.06) c	71.0 (3.9) a

est). *Populus tremuloides* was especially variable in its effect on transpiration, exhibiting the greatest influence on total transpiration when expressed on a per leaf basis, and the least when expressed on a per tree basis. The sample size for each species reflects the presence of that species, with *P. tremuloides*, *P. contorta* and *A. lasiocarpa* present throughout the hill slope and *P. engelmannii* present almost exclusively in the lower-slope area (Figure 1).

### Half-hourly transpiration and environmental drivers

Species effects on transpiration are often dynamic not only because of biomass partitioning between sapwood area and leaf area, as noted above, but because of dynamic interaction with atmospheric drivers. Figure 2 further illustrates the effect of species on transpiration expressed as  $J_S$ ,  $E_C$  or  $E_L$  with time. As observed in an emerging group of studies (summarized by Dawson et al. 2007), transpiration and  $D$  are often nonzero at night ( $Q < 10 \mu\text{mol m}^{-2} \text{ s}^{-1}$ ). Peak midday values for  $E_L$  could be consistently ranked as *P. tremuloides* > *P. contorta* > *P. engelmannii* > *A. lasiocarpa*. Ordering of peak values for  $E_C$  were also consistent across time, with *P. contorta* > *P. engelmannii* > *A. lasiocarpa* > *P. tremuloides*. These rankings were consistent across the entire dataset with the magnitude of the differences increasing with increasing values of  $D$  and  $Q$  (Figure 3). There were strong correlations ( $P < 0.001$  for all) between  $D$  and transpiration at all scales ( $J_S$ ,  $E_L$  and  $E_C$ ;  $r^2 = 0.83$  for all species), species-specific sap flow and transpiration ( $r^2$  ranged from 0.81 to 0.83) and  $Q$  ( $r^2 = 0.87$ ). Based on a visual verification of best residual distribution, the relationships between transpiration and  $Q$  were always linear, whereas all of the conifers showed a saturating response to  $D$  (Figure 3).

### Spatial patterns

Six trees fit all three criteria for outliers (Figure 4) and were excluded from all spatial analyses. The outlying trees were *P. contorta* (four outliers) and *P. engelmannii* (two outliers). There was no exhibited spatial association among geostatistical outliers, nor did they correlate with measured environmental variables including soil water content. Outliers' responses to  $D$  were not significantly different from those of the included trees. Soil water content explained the location of only one outlier, which had an  $A_S$  of  $852.6 \text{ cm}^2$ , almost twice that of the next largest tree and almost three times that of the

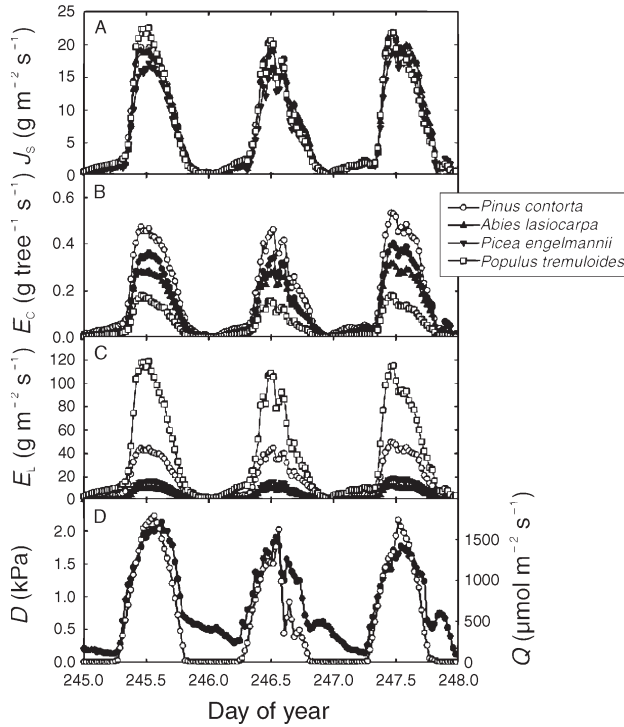


Figure 2. Half-hourly time series over three days of (A) sap flow per unit sapwood area ( $J_s$ ), (B) whole-tree transpiration ( $E_c$ ), (C) transpiration per unit leaf area ( $E_L$ ) and (D) environmental drivers vapor pressure deficit ( $D$ , ●) and photosynthetically active radiation ( $Q$ , ○). Values are species means with samples sizes given in Table 1.

95th percentile. Moreover, the soil water content at that tree's plot center was more than three times the mean percent soil water in the study.

All semivariograms were isotropic, and best modeled by a spherical equation (Equation 4). The requirements for second-order stationarity were met; the drift for all semivariograms had no discernable slope, and neither means nor variances changed spatially. Figure 5 illustrates the effect of including or excluding the deciduous tree species (*P. tremuloides*) when  $D$  is high (2.1 kPa) in semivariograms of transpiration expressed at different scales. When transpiration was expressed as  $J_s$ , the spatial autocorrelation was lowest as indicated by the large ratio between nugget and sill and the shorter range (Figure 5, Table 3). Including or removing *P. tremuloides* from the semivariogram of  $J_s$  had little effect. When transpiration was expressed as  $E_L$ , the ratio between the nugget and sill was much lower than for  $J_s$  and the range was intermediate between  $J_s$  and  $E_c$ . *Populus tremuloides* drastically modified the  $E_L$  spatial patterns. Total variability, expressed as the sill and nugget, was much larger with *P. tremuloides* than without. When transpiration was expressed as  $E_c$ , spatial autocorrelation was highest as measured by the range and the ratio between sill and nugget. Including or removing *P. tremuloides* from the semivariogram of  $E_c$  had no discernable effect. Removing *A. lasiocarpa* or *P. engelmannii* had no discernable effect on any semivariogram. Sample sizes were insufficient to produce semivariograms for individual species. When semi-

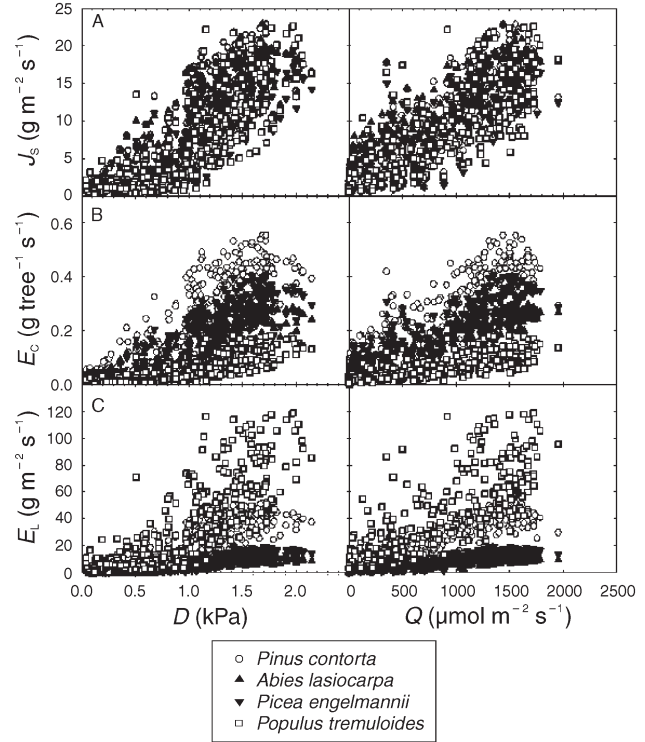


Figure 3. Responses of half-hourly (A) sap flow per unit sapwood area ( $J_s$ ), (B) whole-tree transpiration ( $E_c$ ) and (C) transpiration per unit leaf area ( $E_L$ ) to environmental drivers vapor pressure deficit ( $D$ ) and photosynthetically active radiation ( $Q$ ). Values are species means with samples sizes given in Table 1.

variograms of  $J_s$  were produced at each  $D$  bin, only the highest  $D$  (shown in Figure 5A) had spatial autocorrelation. The  $D$  bins of  $J_s$  less than 2.0 kPa had (1) spatial ranges close to zero, (2) ratio between nugget and sill greater than 0.8, and (3)  $r^2$  values less than 0.15, all indicating no spatial autocorrelation. Across all bins of  $D$ ,  $E_L$  and  $E_c$  had significant spatial auto-

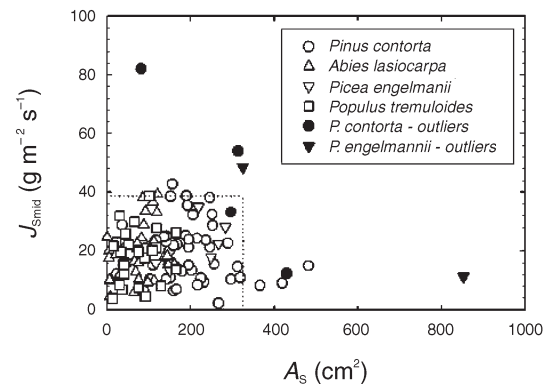


Figure 4. Relationship between midday sap flow per unit sapwood area ( $J_{Smid}$ ) averaged over the dataset and sapwood area per tree ( $A_s$ ). Filled symbols indicate trees that were selected as statistical outliers and removed from spatial analyses based on three conditions detailed in the methods. Dashed lines represent the 95th percentile of  $J_{Smid}$  and  $A_s$  values.

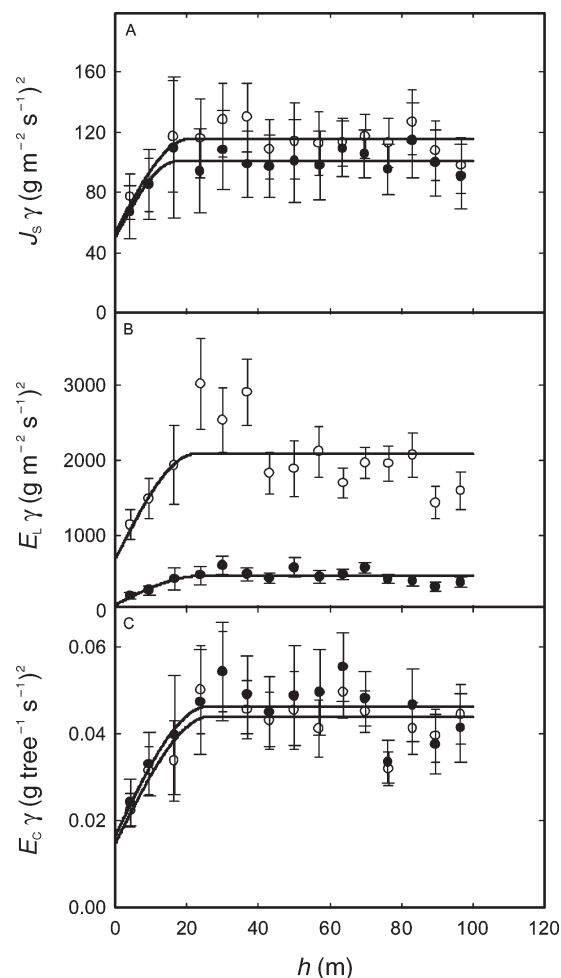


Figure 5. Relationships between semivariance ( $\gamma$ ) of (A) transpiration per unit sapwood area ( $J_s$ ), (B) per unit leaf area ( $E_L$ ) and (C) per tree ( $E_C$ ) and distance between sample point pairs ( $h$ ) with (○) and without (●) *Populus tremuloides*. Values were taken at a vapor pressure deficit of 2.1 kPa, representing the middle of a 0.2-kPa bin. For modeled semivariogram parameters see Table 3.

correlation. Because of the similar patterns with  $D$  bins, only  $E_C$  is described in the next section.

#### Determining temporal drivers of spatial patterns

Figure 6 illustrates the effect of three  $D$  bins (out of 11) on semivariograms of  $E_C$ . The spatial range declined as  $D$  increased, but there was no clear trend in the amount of variability explained by the modeled semivariogram. At low  $D$  (0.5-kPa bin), the range was 44.3 m and the proportion of total variability that was spatial ( $C/(C_0 + C)$ ) was 64%; at mid  $D$  (1.1-kPa bin), the range was 32.8 m and the proportion was 61%; at high  $D$  (2.0-kPa bin), the range was 25.7 m and the proportion was 73%. To test whether this relationship holds across all  $D$  bins, Figure 7 shows the range, sill and nugget of  $E_C$  as a function of  $D$ . The total variability of  $E_C$  increased with increasing  $D$  in a sigmoidal fashion, as expressed by both the nugget ( $r^2 = 0.99$ ) and sill ( $r^2 = 0.98$ ) (Figures 7A and 7B). The range of spatial autocorrelation decreased by a factor of three as  $D$  increased (Figure 7C;  $r^2 = 0.89$ ) reflecting the increasing total variability in  $E_C$ . Half-hourly sap flow values were also binned according to corresponding  $Q$  values, and  $Q$  was tested as a prospective driver of spatial patterns in transpiration, but it explained substantially less variability in the spatial autocorrelation ranges ( $r^2 = 0.64$ ) than  $D$ . When sap flow values were binned by time and semivariogram parameters were plotted as a function of the mean  $D$  for each binned block of time, the range exhibited a stronger correlation ( $r^2 = 0.83$ ).

Point-Kriged maps illustrating the increase in  $E_C$  variability with increasing  $D$  are shown in Figure 8. At a  $D$  bin representing low  $D$  (0.5 kPa; Figure 8A),  $E_C$  was nearly constant with just one area showing a slightly higher value. At a moderate  $D$  bin (1.0 kPa; Figure 8B) variability in  $E_C$  increased with highest values found in the same location as in Figure 8A. At a high  $D$  bin (2.0 kPa; Figure 8C),  $E_C$  variability is visibly greatest with a full mosaic of high and low  $E_C$  throughout the hillslope.

Table 3. Semivariogram parameters for Figures 5 and 6. Abbreviations:  $J_s$ , sap flow per unit sapwood area;  $E_C$ , transpiration per tree;  $E_L$ , transpiration per leaf area;  $D$ , vapor pressure deficit; Ratio, nugget divided by sill; and  $P$ , significance level of the regression. Semivariogram parameters (range, nugget and sill) are taken from fitting Equation 4 to empirical semivariance. Nugget units are  $(\text{g m}^{-2} \text{s}^{-1})^2$  for  $J_s$  and  $E_L$ , and  $(\text{g tree}^{-1} \text{s}^{-1})^2$  for  $E_C$ .

Semivariogram	Range (m)	Nugget	Sill	Ratio	$r^2$	$P$
$J_s$ , with <i>P. tremuloides</i>	20.7	53.7	115.6	0.47	0.65	< 0.05
$J_s$ , without <i>P. tremuloides</i>	17.0	50.2	100.2	0.50	0.68	< 0.05
$E_L$ , with <i>P. tremuloides</i>	22.3	683	2081	0.33	0.28	< 0.05
$E_L$ , without <i>P. tremuloides</i>	24.2	76	458	0.17	0.53	< 0.05
$E_C$ , with <i>P. tremuloides</i>	26.5	0.015	0.045	0.34	0.60	< 0.001
$E_C$ , without <i>P. tremuloides</i>	25.9	0.016	0.047	0.36	0.57	< 0.01
$E_C$ , $D = 0.5$ kPa	44.3	0.0001	0.0003	0.35	0.51	< 0.01
$E_C$ , $D = 1.1$ kPa	32.0	0.005	0.013	0.39	0.72	< 0.001
$E_C$ , $D = 2.1$ kPa	25.7	0.012	0.047	0.27	0.56	< 0.001

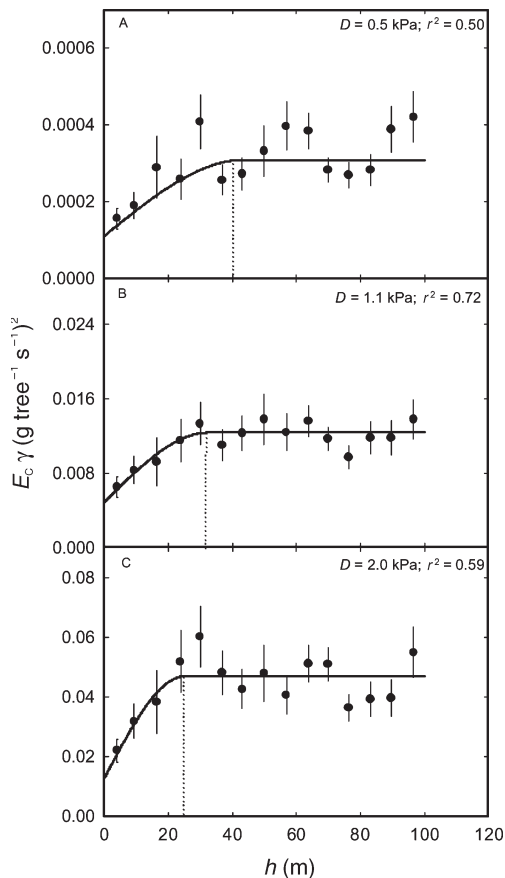


Figure 6. Relationship between semivariance ( $\gamma$ ) of whole-tree transpiration ( $E_C$ ) and distance between sample point pairs ( $h$ ) for three vapor pressure deficit ( $D$ ) bins at (A) 0.5 kPa, (B) 1.1 kPa and (C) 2.0 kPa. Each value of  $D$  represents the middle of a 0.2-kPa bin. Dotted lines represent semivariogram ranges calculated using weighted regression on Equation 4; see Table 3 for parameters of the modeled semivariograms.

## Discussion

Data from this study supported all three hypotheses: (1) spatial structure exists in transpiration; (2) spatial structure of transpiration varies temporally; and (3) an environmental variable, namely  $D$ , drives temporal dynamics in this spatial structure. Spatial patterns of transpiration are dynamic. When  $D$  is low (early morning or late afternoon) there is less spatial variability, and the range at which spatial autocorrelation occurs is greatest. When  $D$  is high (midday), transpiration is more variable and spatial autocorrelation occurs at smaller distances.

### Environmental and species effects on transpiration

Temporal dynamics in transpiration are often best explained by  $D$  for many species (Schulze et al. 1985, Monteith 1995, Phillips et al. 1997) including the four species from this study (Pataki et al. 2000). The transpiration response to  $D$  is strongest when trees are well coupled to the atmosphere. Such situations are often found in conifers, small-leaved trees and high wind areas, all of which are characteristic of the study site and

further indicate that  $D$  is not spatially variable within the canopy across the stand (Jarvis and McNaughton 1986). The response of transpiration to  $D$  reflects tree hydraulic capacity to transport available water (Oren et al. 1999, Ewers et al. 2000). Thus, all trees exhibit a linear response to low  $D$ , whereas at high  $D$ , low leaf water potentials and the potential for excessive cavitation lead to stomatal closure and a saturating response of transpiration to  $D$  in many trees (Sperry et al. 1998, Oren et al. 1999, Pataki et al. 2000; see Ewers et al. 2005 for important exceptions). On a diel basis, this response to high  $D$ , can be masked by short-term light dynamics from self-shading, penumbral effects and the amount of diffuse versus direct sunlight, and thus requires smoothing of the transpiration data in time (Ewers et al. 2007).

The effect of species on transpiration is a combination of biomass partitioning between  $A_S$  and  $A_L$  (McDowell et al. 2002) and differential stomatal conductance response to  $D$  (Mott and Parkhurst 1991, Oren et al. 1999). Hydraulic theory predicts that sapwood-to-leaf area ratios will increase as trees increase in size to compensate for height effects; however certain trees, such as those in the *Picea* and *Abies* genera, have opposite trends (McDowell et al. 2002) and a corresponding difference in the transpiration/stomatal conductance response to  $D$  (Ewers et al. 2005). In this study, neither *A. lasiocarpa* nor *P. engelmannii* displayed a linear relationship between  $D$  and transpiration, probably reflecting the relatively young age and small size of the stand and subsequent lack of significant height effects on tree hydraulics as hypothesized by Ewers et al. (2005). Thus, the spatial differences in transpiration found in this study are likely more the result of spatial changes in  $A_S$  and  $A_L$  across the stand than unrelated species differences.

The method of binning transpiration by  $D$  values in this study removes high frequency noise unrelated to plant hydraulics (Ewers et al. 2007) thus allowing robust spatial analyses of transpiration at each  $D$  bin. The transpiration response of the tree species to  $D$  (Figures 2 and 3) is the same as that reported by Pataki et al. (2000). Although slope position had no effect on transpiration, species had significant effects on  $E_C$  and  $E_L$  (Table 2; Figures 2 and 3). The lack of an effect of slope position may be because measurements were made late in the season when soil water content was already low throughout the slope. Consistent with this interpretation, the stream had dried up by the time of the measurements. However, we cannot rule out long-term effects of hill-slope position (Tromp-van Meerveld and McDonnell 2006). The greater abundance of *P. engelmannii* and *A. lasiocarpa* on the lower slope, both of which use water less efficiently than other tree species in the region (Knapp and Smith 1981), implies an effect of hill-slope position on establishment and mature tree physiology.

One source of possible error in our sap flow and scaled transpiration values is the lack of quantified radial and circumferential trends because of power failures during the sap flow measurements. The literature contains many studies detailing the importance of these trends (Phillips et al. 1996, Oren et al. 1998, Ewers and Oren 2000, Lu et al. 2000, Lundblad et al. 2001, Ewers et al. 2002, James et al. 2002). In our study, because an average of more than 75% of the sapwood depth, was

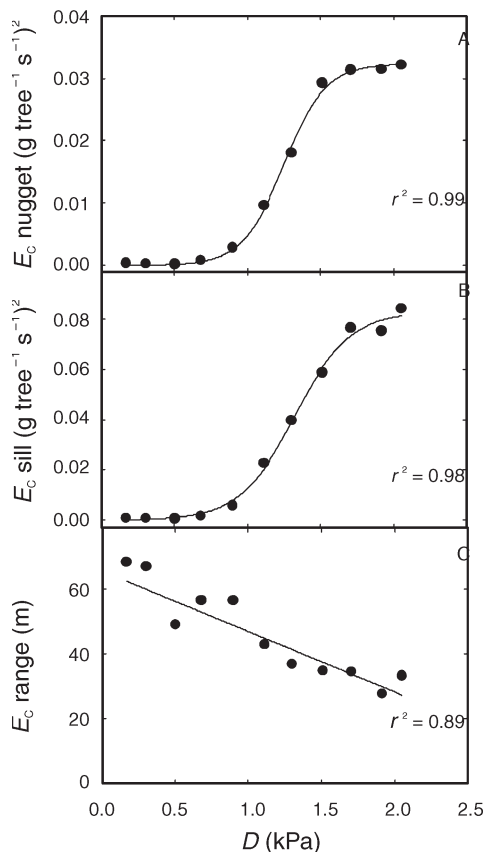


Figure 7. Relationships between semivariogram parameters (Equation 5) (A) nugget, (B) sill and (C) range of whole-tree transpiration ( $E_C$ ) and vapor pressure deficit ( $D$ ) across all eleven 0.2-kPa  $D$  bins.

accounted for in the sap flow measurements, this error should be minimal.

Another potential source of error is the series of allometric equations used to estimate leaf area. Although these equations were locally derived and included the full range of tree sizes in the study (Kaufmann and Troedle 1981), it is unlikely that the allometric relationships are constant in space. Studies have shown changes in  $A_S$  to  $A_L$  area relationships with tree size

(McDowell et al. 2002), stand development (Coyea and Margolis 1992, Magnani et al. 2000), and edaphic conditions such as nutrient and water availability (Ewers et al. 2000). Our results suggest, however, that the allometric changes within a species were negligible, because there was no effect of slope position on transpiration and stand development was similar throughout the spatial sampling area. Any effect of changing allometrics is thus likely to be random and not spatially dependent, although this assumption has not been verified.

*Spatial structure of transpiration*

Six trees were identified as outliers; this constitutes less than 4.5% of the total number of sap flow sensor pairs. One frequent rationale for removing an outlier is the sensitivity of semivariograms to extreme values relative to the mean of a population (Cressie 1993). In this case, the six statistical outliers may also be physiological outliers (Figure 2)—although none of them showed a significantly different response to  $D$  from the included trees—or methodological outliers. Traditional sampling may find no extreme values because (1) the sample size is small and (2) measurements are clustered within “representative plots” and may not capture the full range of variability (Oren et al. 1998). The outliers may reflect trees responding to different soil water sources; the outliers all represent very large fluxes for their size or are the biggest trees measured, or both (Figure 4). These trees may be able to tap into more stable groundwater sources (Dawson and Ehleringer 1991), but we did not investigate this possibility.

Despite the size of the particular study, there were too few sensor pairs in three of the four species to conduct species-specific analyses of spatial autocorrelation. When comparing  $E_L$  with all species included and with *P. tremuloides* excluded, semivariogram parameters differed (Figure 5). The range of the semivariogram of  $J_S$  is close to zero unless  $D$  is high, and that of the semivariogram of  $E_L$ —where  $A_L$  is an additional informing variable (see Equation 1)—is little different from the range of  $E_C$  semivariogram (Figure 5). The main increase in spatial structure, therefore, can be attributed to  $A_S$ , which is the lone variable that distinguishes transpiration on a per tree basis from  $J_S$  (see Equation 2).

Another limitation of the study is its short duration relative

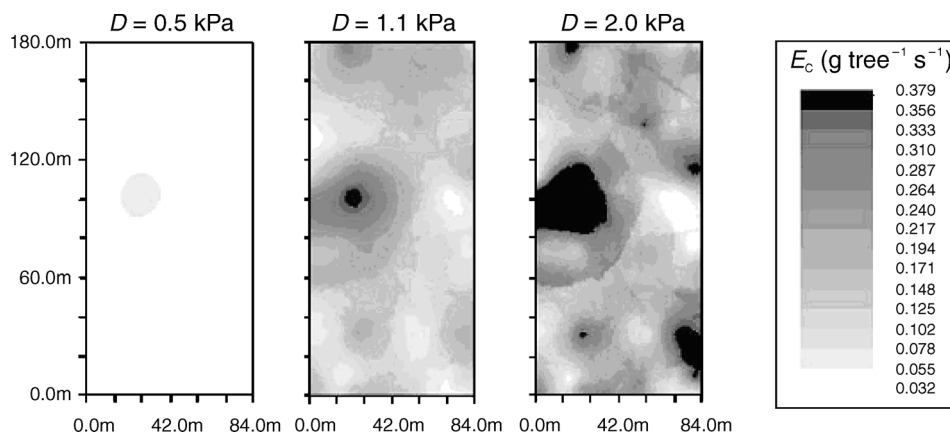


Figure 8. Point-Kriged maps of whole-tree transpiration ( $E_C$ ) at vapor pressure deficit ( $D$ ) bins of 0.5, 1.1 and 2.0 kPa. Each value of  $D$  represents the middle of a 0.2-kPa bin.

to the length of the growing season. Furthermore, because this study took place during the period of minimal soil water content (early August to the end of the growing season; Pataki et al. 2000), the results may have been quite different if the study had been conducted during the early part of the growing season. Immediately following snowmelt, all hill-slope positions are likely to have the same relative soil water content if the snowpack is sufficient to saturate the entire rooting zone (Knight et al. 1985). Spatial autocorrelation in soil water content would thus be extremely high and combined with low  $D$  from low air temperatures would create a scenario of perhaps higher spatial autocorrelation than was reported here. If the snowpack is insufficient for soil saturation or the soil water content is reduced by root uptake, spatial patterns in soil water content will be more manifest, providing feedback to tree transpiration at a given  $D$  as found in a recent hill-slope study of tree transpiration (Tromp-van Meerveld and McDonnell 2006). These interacting spatial patterns in soil water content and tree transpiration would then become minimal as the growing season progresses and soil water content declines leading to the conclusion that our study period may be biased by more spatial autocorrelation than would exist when soil water content is at an intermediate value.

#### *Temporal dynamics of transpiration spatial structure*

Differences in  $D$  explain differences in time not only for traditional analyses of transpiration, but also for geostatistical analyses; the range of  $E_C$  semivariograms decreased progressively with  $D$  (Figure 7). Kriging (Figure 8) from semivariograms (Figure 6) showed not only major changes in values and spatial structure of transpiration, but also progressively smaller areas of uniform  $E_C$  with increasing  $D$ . This correlation between  $D$  and spatial autocorrelation can be observed quantitatively with changes in semivariogram parameters (Figure 7, Table 3). The total variability increases with  $D$ ; however, the sill and nugget change in parallel, so that the nugget-to-sill ratio is constant with a mean of 0.4. This ratio appears to be hovering around the proposed ratio of significance (Lopez-Granados et al. 2004) for semivariograms; i.e., the nugget-to-sill ratio is generally 0.4 or less if the spatial pattern being observed has biological relevance. Thus, if  $D$  were to continue to increase, spatial autocorrelation in transpiration could be lost as a result of the decreasing range of spatial autocorrelation in the stand.

Other variables were tested to see if, and how well, they explain spatial patterns of transpiration. The inability of  $Q$  to predict changes in semivariogram parameters is ecologically intelligible; transpiration in these species is driven by changes in  $D$  (Pataki et al. 2000) because they are well coupled to the atmosphere (Jarvis and McNaughton 1986). When  $E_C$  values were binned by time instead of  $D$ , semivariogram parameters and corresponding spatial patterns were explained less well than when  $E_C$  was binned by  $D$ .

Even with the potential hydraulic explanation for  $D$  effects on spatial patterning, this study provides no definitive explanation for the precise clustering of tree transpiration at high  $D$  (Figure 8). Several speculative explanations worth future ex-

ploration include the following. Genetic autocorrelation may occur in space as a result of factors such as clustering of similar individuals resulting from the amount of *P. contorta* serotiny in response to fires and squirrels (Benkman and Siepielski 2004) or clonal propagation (e.g., Huenneke 1985) of *P. tremuloides* and *A. lasiocarpa*. Acclimation to edaphic conditions such as plant hydraulic responses to soil texture changes (Hacke et al. 2000) may also cause transpiration autocorrelation as a result of soil textural changes across a hill slope.

Our results indicate that stand transpiration can be scaled and modeled from a small sample of trees if (1) the responses to  $D$  of those trees are representative and can thus be explained hydraulically and (2) the rate of change in range, sill and nugget can be predicted from tree hydraulics. This study offers a methodology that attempts to overcome the constraints that space and time impose on each other in ecosystems. One implication of this study is the need to find easily measured proxies that can determine spatial structure. These proxies can be ground-based (DBH, basal area; Moisen et al. 2006) for stand-level measurements or derived from remotely sensed data (stand density, leaf area index) for larger areas (Berterretche et al. 2005). If the hypothesized process (i.e., tree hydraulics) underlying the patterns observed in this study is supported in other ecosystems, there is no longer a need to deal with transpiration's spatial autocorrelation. Future studies can utilize process explanations instead of partially unexplained variability, an approach that can be applied broadly to ecosystem studies.

#### **Acknowledgments**

This research was partially supported by the NSF Hydrologic Sciences Program through Grants EAR-0405306 and EAR-0405381, and by Wyoming NASA Space Grant Consortium and Wyoming NASA EPSCoR through Grants NGT-40102 and NCC-578, respectively. Sarah Adelman, Ian Abernathy, Melody Durrett, Luitgardt Schwendenmann and Elise Pendall provided invaluable field and laboratory assistance. Dave Williams and Scott Miller provided comments that improved an earlier version of the paper.

#### **References**

- Anderson, T.M., S.J. McNaughton and M.E. Ritchie. 2004. Scale-dependent relationships between the spatial distribution of a limiting resource and plant species diversity in an African grassland ecosystem. *Oecologia* 139:277–287.
- Ball, J.T., I.E. Woodrow and J.A. Berry. 1987. A model predicting stomatal conductance and its contribution to the control of photosynthesis under different environmental conditions. *Prog. Photosynth. Res.* 4:221–224.
- Benkman, C.W. and A.M. Siepielski. 2004. A keystone selective agent? Pine squirrels and the frequency of serotiny in lodgepole pine. *Ecology* 85:2082–2087.
- Berterretche, M., A.T. Hudak, W.B. Cohen, T.K. Maiersperger, S.T. Gower and J. Dungan. 2005. Comparison of regression and geostatistical methods for mapping Leaf Area Index (LAI) with Landsat ETM+ data over a boreal forest. *Remote Sens. Environ.* 96:49–61.
- Bishop, M.P., J.F. Shroder and J.D. Colby. 2003. Remote sensing and geomorphology for studying relief production in high mountains. *Geomorphology* 55:345–361.

- Burrows, S.N., S.T. Gower, M.K. Clayton, D.S. Mackay, D.E. Ahl, J.M. Norman and G. Diak. 2002. Application of geostatistics to characterize leaf area index (LAI) from flux tower to landscape scales using a cyclic sampling design. *Ecosystems* 5:667–679.
- Carter, G.A. and W.K. Smith. 1988. Microhabitat comparisons of transpiration and photosynthesis in three subalpine conifers. *Can. J. Bot.* 66:963–969.
- Čermák, J., E. Cienciala, J. Kučera, A. Lindroth and E. Bednárová. 1995. Individual variation in sap-flow rate in large pine and spruce trees and stand transpiration: a pilot study at the central NOPEX site. *J. Hydrol.* 168:17–27.
- Chang, C.R., P.F. Lee, M.L. Bai and T.T. Lin. 2006. Identifying the scale thresholds for field-data extrapolation via spatial analysis of landscape gradients. *Ecosystems* 9:200–214.
- Clearwater, M.J., F.C. Meinzer, J.L. Andrade, G. Goldstein and N.M. Holbrook. 1999. Potential errors in measurement of nonuniform sap flow using heat dissipation probes. *Tree Physiol.* 19:681–687.
- Conti, D.V. and J.S. Witte. 2003. Hierarchical modeling of linkage disequilibrium: genetic structure and spatial relations. *Am. J. Hum. Genet.* 72:351–363.
- Coyea, M.R. and H.A. Margolis. 1992. Factors affecting the relationship between sapwood area and leaf area of balsam fir. *Can. J. For. Res.* 22:1684–1693.
- Cressie, N.A.C. 1993. *Statistics for spatial data*. Revised Edn. John Wiley and Sons, New York, 900 p.
- Dawson, T.E. and J.R. Ehleringer. 1991. Streamside trees that do not use stream water. *Nature* 350:335–337.
- Dawson, T.E., S.S.O. Burgess, K.P. Tu, R.S. Oliveira, L.S. Santiago, J.B. Fisher, K.A. Simonin and A.R. Ambrose. 2007. Nighttime transpiration in woody plants from contrasting ecosystems. *Tree Physiol.* 27:561–575.
- Day, T.A., E.H. DeLucia and W.K. Smith. 1987. Influences of cold soil and snow cover on photosynthesis and leaf conductance in two Rocky Mountain conifers. *Oecologia* 80:546–552.
- Dewar, R.C. 2002. The Ball-Berry-Leuning and Tardieu-Davies stomatal models: synthesis and extension within a spatially aggregated picture of guard cell function. *Plant Cell Environ.* 25:1388–1398.
- Ewers, B.E. and R. Oren. 2000. Analyses of assumptions and errors in the calculation of stomatal conductance from sap flux measurements. *Tree Physiol.* 20:579–589.
- Ewers, B.E., R. Oren and J.S. Sperry. 2000. Influence of nutrient versus water supply on hydraulic architecture and water balance in *Pinus taeda*. *Plant Cell Environ.* 23:1055–1066.
- Ewers, B.E., D.S. Mackay, S.T. Gower, D.E. Ahl, S.N. Burrows and S.S. Samanta. 2002. Tree species effects on stand transpiration in northern Wisconsin. *Water Resour. Res.* 38(7):10.1029/2001WR000830.
- Ewers, B.E., S.T. Gower, B. Bond-Lamberty and C.K. Wang. 2005. Effects of stand age and tree species on canopy transpiration and average stomatal conductance of boreal forests. *Plant Cell Environ.* 28:660–678.
- Ewers, B.E., R. Oren, H.-S. Kim, G. Bohrer and C.T. Lai. 2007. Effects of hydraulic architecture and spatial variation in light on mean stomatal conductance of tree branches and crowns. *Plant Cell Environ.* 30:483–496.
- Fahey, T.J. and D.R. Young. 1984. Soil and xylem water potential and soil water content in contrasting *Pinus contorta* ecosystems. *Oecologia* 61:346–351.
- Farquhar, G.D. and S.C. Wong. 1984. An empirical model of stomatal conductance. *Aust. J. Plant Physiol.* 11:191–210.
- Fetcher, N. 1976. Patterns of leaf resistance to lodgepole pine transpiration in Wyoming. *Ecology* 57:339–345.
- Franklin, R.B., L.K. Blum, A.C. McComb and A.L. Mills. 2002. A geostatistical analysis of small-scale spatial variability in bacterial abundance and community structure in salt marsh creek bank sediments. *FEMS Microbiol. Ecol.* 42:71–80.
- Granier, A. 1987. Evaluation of transpiration in a Douglas fir stand by means of sap flow measurements. *Tree Physiol.* 3:309–320.
- Granier, A., P. Biron, N. Brèda, J.Y. Pontailler and B. Saugier. 1996. Transpiration of trees and forest stands: short and long-term monitoring using sapflow methods. *Global Change Biol.* 2:265–274.
- Hacke, U.G., J.S. Sperry, B.E. Ewers, D.S. Ellsworth, K.V.R. Schafer and R. Oren. 2000. Influence of soil porosity on water use in *Pinus taeda*. *Oecologia* 124:495–505.
- Huenneke, L.F. 1985. Spatial-distribution of genetic individuals in thickets of *Alnus incana* ssp. *rugosa*, a clonal shrub. *Am. J. Bot.* 72:152–158.
- Isaaks, E.H. and R.M. Srivastava. 1989. *An introduction to applied geostatistics*. Oxford University Press, New York, 561 p.
- Jackson, R.B. and M.M. Caldwell. 1993. The scale of nutrient heterogeneity around individual plants and its quantification with geostatistics. *Ecology* 74:612–614.
- James, S.A., M.J. Clearwater, F.C. Meinzer and G. Goldstein. 2002. Heat dissipation sensors of variable length for the measurement of sap flow in trees with deep sapwood. *Tree Physiol.* 22:277–283.
- Jarvis, P.G. 1976. The interpretation of the variations in leaf water potential and stomatal conductance found in canopies in the field. *Philos. Trans. R. Soc. Lond. Biol. Sci.* 273:593–610.
- Jarvis, P.G. 1995. Scaling processes and problems. *Plant Cell Environ.* 18:1079–1089.
- Jarvis, P.G. and K.G. McNaughton. 1986. Stomatal control of transpiration: scaling up from leaf to region. *Adv. Ecol. Res.* 15:1–50.
- Kaluzny, S.P., S.C. Vega, T.P. Cardoso and A.A. Shelly. 1998. *S+ spatial stats: user's manual for Windows and Unix*. Springer-Verlag, New York, 327 p.
- Kaufmann, M.R. 1985. Annual transpiration in subalpine forests: large differences among four tree species. *For. Ecol. Manage.* 13:235–246.
- Kaufmann, M.R. and C.A. Troendle. 1981. The relationship of leaf area and foliage biomass to sapwood conducting area in four subalpine forest trees. *For. Sci.* 27:477–482.
- Knapp, A.K. and W.K. Smith. 1981. Water relations and succession in subalpine conifers in southeastern Wyoming. *Bot. Gaz.* 142:502–511.
- Knight, D.H., T.J. Fahey, S.W. Running, A.T. Harrison and L.L. Wallace. 1981. Transpiration from 100-year-old lodgepole pine forests estimated with whole-tree potometers. *Ecology* 62:717–726.
- Knight, D.H., T.J. Fahey and S.W. Running. 1985. Water and nutrient outflow from contrasting lodgepole pine forests in Wyoming. *Ecol. Monogr.* 55:29–48.
- Legendre, P. 1993. Spatial autocorrelation: trouble or new paradigm? *Ecology* 74:1659–1673.
- Legendre, P. and L. Legendre. 1998. *Numerical ecology*. 2nd English Edn. Elsevier Science BV, Amsterdam, 853 p.
- Leuning, R. 1995. A critical appraisal of a combined stomatal-photosynthesis model. *Plant Cell Environ.* 18:339–355.
- Levin, S.A. 1992. The problem of pattern and scale in ecology. *Ecology* 73:1943–1967.
- Lopez-Granados, F., M. Jurado-Exposito, S. Alamo and L. Garcia-Torres. 2004. Leaf nutrient spatial variability and site-specific fertilization maps within olive (*Olea europaea* L.) orchards. *Eur. J. Agron.* 21:209–222.

- Lu, P., W.J. Muller and E.K. Chacko. 2000. Spatial variations in xylem sap flux density in the trunk of orchard-grown, mature mango trees under changing soil water conditions. *Tree Physiol.* 20: 683–692.
- Lundblad, M., F. Lagergren and A. Lindroth. 2001. Evaluation of heat balance and heat dissipation methods for sapflow measurements in pine and spruce. *Ann. Sci. For.* 58:625–638.
- Magnani, F., M. Mencuccini and J. Grace. 2000. Age-related decline in stand productivity: the role of structural acclimation under hydraulic constraints. *Plant Cell Environ.* 23:251–263.
- McDowell, N.G., H. Barnard, B.J. Bon et al. 2002. The relationship between tree height and leaf area:sapwood area ratio. *Oecologia* 132:12–20.
- Moisen, G.G., E.A. Freeman, J.A. Blackard, T.S. Frescino, N.E. Zimmerman and T.C. Edwards, Jr. 2006. Predicting tree species presence and basal area in Utah: a comparison of stochastic gradient boosting, generalized additive models and tree-based estimates. *Ecol. Model.* 199:176–187.
- Monteith, J.L. 1995. A reinterpretation of stomatal response to humidity. *Plant Cell Environ.* 18:357–364.
- Morris, S.J. 1999. Spatial distribution of fungal and bacterial biomass in southern Ohio hardwood forest soils: fine scale variability and microscale patterns. *Soil Biol. Biochem.* 31:1375–1386.
- Mott, K.A. and D.F. Parkhurst. 1991. Stomatal response to humidity in air and helox. *Plant Cell Environ.* 14:509–515.
- Neuhauser, C. 2001. Mathematical challenges in spatial ecology. *Notices Am. Math. Soc.* 48:1304–1314.
- Oren, R., N. Phillips, G. Katul, B.E. Ewers and D.E. Pataki. 1998. Scaling xylem sap flux and soil water balance and calculating variance: a method for partitioning water flux in forests. *Ann. Sci. For.* 55:191–216.
- Oren, R., J.S. Sperry, G.G. Katul, D.E. Pataki, B.E. Ewers, N. Phillips and K.V.R. Schafer. 1999. Survey and synthesis of intra- and interspecific variation in stomatal sensitivity to vapour pressure deficit. *Plant Cell Environ.* 22:1515–1526.
- Pataki, D.E., R. Oren and W. Smith. 2000. Sap flux of co-occurring species in a western subalpine forest during seasonal drought. *Ecology* 81:2557–2566.
- Phillips, N., R. Oren and R. Zimmermann. 1996. Radial patterns of xylem sap flow in non-, diffuse- and ring-porous tree species. *Plant Cell Environ.* 19:983–990.
- Phillips, N., A. Nagchadhuri, R. Oren and G. Katul. 1997. Time constant for water transport in loblolly pine trees estimated from time series of evaporative demand and stem sapflow. *Trees* 11:412–419.
- Pinheiro, J. and D. Bates. 2000. *Mixed-effects models in S and S-Plus*. Springer-Verlag, New York, 528 p.
- Rahman, S., L.C. Munn, R. Zhang and G.F. Vance. 1996. Rocky Mountain forest soils: evaluating spatial variability using conventional statistics and geostatistics. *Can. J. Soil. Sci.* 76:501–507.
- Robertson, G.P. 1987. Geostatistics in ecology: interpolating with known variance. *Ecology* 68:744–748.
- Running, S.W. 1980a. Environmental and physiological control of water flux through *Pinus contorta*. *Can. J. For. Res.* 10:82–91.
- Running, S.W. 1980b. Field estimates of root and xylem resistances in *Pinus contorta* using root excision. *J. Exp. Bot.* 31:555–569.
- Schabenberger, O. and C.A. Gotway. 2004. *Statistical methods for spatial data analysis*, CRC Press, Boca Raton, FL, 488 p.
- Scheidegger, A.E. 1974. *The physics of flow through porous media*. 3rd Edn. University of Toronto Press, Toronto, 353 p.
- Schlesinger, W.H., J.A. Raikes, A.E. Hartley and A.F. Cross. 1996. On the spatial pattern of soil nutrients in desert ecosystems. *Ecology* 77:364–374.
- Schulze, E.-D., J. Čermák, R. Matyssek, M. Penka, R. Zimmerman, F. Vasicek, W. Gries and J. Kučera. 1985. Canopy transpiration and water fluxes in the xylem of the trunk of *Larix* and *Picea* trees—a comparison of xylem flow, porometer and cuvette measurements. *Oecologia* 66:475–483.
- Smith, W.K., D.R. Young, G.A. Carter, J.L. Hadley and G.M. McNaughton. 1984. Autumn stomatal closure in six conifer species of the central Rocky Mountains. *Oecologia* 63:237–242.
- Sokal, R.R. and F.J. Rohlf. 1995. *Biometry: the principles and practice of statistics in biological research*. 3rd Edn. W.H. Freeman and Co., New York, 887 p.
- Sperry, J.S., F.R. Adler, G.S. Campbell and J.P. Comstock. 1998. Limitation of plant water use by rhizosphere and xylem conductance: results from a model. *Plant Cell Environ.* 21:347–359.
- Tang, J., P.V. Bolstad, B.E. Ewers, A.R. Desai and K.J. Davis. 2006. Sap flux upscaled canopy transpiration, stomatal conductance and water use efficiency in an old-growth forest in the Great Lakes region of United States. *J. Geophys. Res.* 111:G02009, doi:10.1029/2005JG000083.
- Tardieu, F. and W.J. Davies. 1993. Integration of hydraulic and chemical signaling in the control of stomatal conductance and water status of droughted plants. *Plant Cell Environ.* 16:341–349.
- Tromp-van Meerveld, H.J. and J.J. McDonnell. 2006. On the interrelations between topography, soil depth, soil moisture, transpiration rates and species distribution at the hillslope scale. *Adv. Water Resour.* 29:293–310.
- Webster, R. and C.H.E. de la Cuanalo. 1975. Soil transect correlograms of north Oxfordshire and their interpretation. *J. Soil. Sci.* 26:176–194.
- Western, A.W., G. Blöschl and R.B. Grayson. 1998. Geostatistical characterisation of soil moisture patterns in the Tarrawarra catchment. *J. Hydrol.* 205:20–37.
- Whitehead, D. and P.G. Jarvis. 1981. Coniferous forests and plantations. *In* *Water Deficits and Plant Growth*, Vol. VI. Ed. T.T. Kozlowski. Academic Press, New York, pp 49–132.
- Wilson, D.J., A.W. Western, R.B. Grayson, A.A. Berg, M.S. Lear, M. Rodell, J.S. Famiglietti, R.A. Woods and T.A. McMahon. 2003. Spatial distribution of soil moisture over 6 and 30 cm depth, Mahurangi river catchment, New Zealand. *J. Hydrol.* 276: 254–274.
- Wullschlegel, S.D., F.C. Meinzer and R.A. Vertessy. 1998. A review of whole-plant water use studies in trees. *Tree Physiol.* 18: 495–512.
- Zweifel, R., J.P. Böhm and R. Häsler. 2002. Midday stomatal closure in Norway spruce—reactions in the upper and lower crown. *Tree Physiol.* 22:1125–1136.